width of a pair of such vortices is shown by the solid curve. In spite of the oversimplification inherent in the proposed model, the intersection of the two curves in Fig. 2 at the experimental critical width indicates very good agreement and similar agreement is obtained for tin films at their much lower critical current density for which the corresponding width is about 2μ.

The suggested relation between the vortex size and critical film width can also account for the observation of the "training" phenomenon in films of width greater than the critical value. The number of quenching trials needed to achieve the maximum critical current in wide films tended to increase with film width, as might be expected in view of the larger number of possible vortex arrangements in the wider films. On the other hand, "training" was never observed in films of less than the critical width. The use of very small samples, therefore, may offer special advantages for thin-film experiments in which the presence of flux vortices severely complicates the interpretation of results.

PHYSICAL REVIEW VOLUME 151, NUMBER 1 4 NOVEMBER 1966

Energy Exchanges Attending Field Electron Emission

L. W. SWANSON, L. C. CROUSER, AND F. M. CHARBONNIER
Field Emission Corporation, McMinnville, Oregon
(Received 23 June 1966)

The energy exchange attending field electron emission (Nottingham effect) is shown to be localized to the emitting area of the cathode. It is further shown that the magnitude and direction (i.e., heating or cooling) depend strongly on cathode temperature, work function, and applied electric field. The temperature boundary separating emission cooling and heating is considerably below theoretical expectations for clean and for zirconium-oxygen-coated tungsten. The existing theory of the Nottingham effect, examined in the light of these and other results, must be modified to include the variation of average energy of the conducting carriers with temperature and field.

I. INTRODUCTION

ELECTRON emission is accompanied by energy exchanges between the conduction electrons and lattice, which become particularly important at the very high emission densities feasible with field and thermal-field (T-F) emission cathodes. Their study is of basic interest since it provides a complementary check, through a direct measurement of the average energy of emitted electrons, of the theory of field and T-F emission; it is also of practical importance because these energy exchanges control the cathode-emitter-tip temperature and set an upper limit on the feasible emission density. The work reported herein is an attempt to confirm, by direct measurement of the energy exchange, the theoretically predicted temperature dependence of the energy exchange and the reversal of its direction (from cathode heating to cooling) at high emitter temperatures.

There are two main emission-induced energy-exchange phenomena. The familiar resistive Joule heating effect was studied in the case of field emission by Dyke *et al.*[1] and Dolan, Dyke, and Trolan.[2] In the usual case where resistivity increases rapidly with temperature, resistive heating by itself leads to an inherently unstable situation at high emission densities. Since stable high-density emission is observed,[3] there must exist another factor having a strong and stabilizing influence on the cathode-tip temperature.

Such a stabilizing factor is provided by the energy exchange resulting from the difference between the average energy of the emitted electrons $\langle E\rangle$ and that of the replacement electron supplied from the Fermi sea, $\langle E'\rangle$. In the case of thermionic emission this phenomenon, discussed by Richardson[4] and later by Nottingham,[5] is well known and produces cooling of a cathode with a work function ϕ by an average energy amount $e\phi+2kT$ per emitted electron. The corresponding effect in field and T-F emission was first discussed by Fleming and Henderson,[6] who were unable to detect it experimentally, and has been a subject of controversy[5,6] with respect to the correct value of $\langle E'\rangle$ and hence the direction of the effect (cathode cooling occurs when $\langle E\rangle>\langle E'\rangle$, and heating when $\langle E\rangle<\langle E'\rangle$). Preliminary data reported earlier[7] tended to support the view of Nottingham who took $\langle E'\rangle$ to be the Fermi energy E_f and, on that basis, predicted heating of the cathode in the case of field emission. Thus, the energy exchange

[1] W. P. Dyke, J. K. Trolan, E. E. Martin, and J. P. Barbour, Phys. Rev. **91**, 1043 (1953).
[2] W. W. Dolan, W. P. Dyke, and J. K. Trolan, Phys. Rev. **91**, 1054 (1953).
[3] E. E. Martin, J. K. Trolan, and W. P. Dyke, J. Appl. Phys. **31**, 782 (1960).
[4] O. A. Richardson, Phil. Trans. Roy. Soc. London **A201**, 497 (1903).
[5] W. B. Nottingham, Phys. Rev. **59**, 907 (1941).
[6] J. E. Henderson and G. M. Fleming, Phys. Rev. **48**, 486 (1935); **54**, 241 (1938); **58**, 908 (1941).
[7] F. M. Charbonnier, R. W. Strayer, L. W. Swanson, and E. E. Martin, Phys. Rev. Letters **13**, 397 (1964).

corresponding to the replacement electron at energy E_f will be referred to as the "Nottingham effect". The new experimental results discussed below for tungsten indicate that $\langle E' \rangle \neq E_f$, seeming at first glance to support the view of Fleming and Henderson. However, this agreement is thought to be fortuitous and the observed difference between $\langle E' \rangle$ and E_f is attributed to the fact that conduction processes in tungsten are not well described by the free-electron model.

The combined effect of resistive and Nottingham phenomena has been treated in the special case of tungsten field emitters initially at room temperature[8]; this work was later extended to other work functions and confirmed experimentally.[9] Levine[10] gave a theoretical analysis of a similar problem. Drechsler[11,12] has reported both departure and agreement with theoretical predictions for the temperature dependence of the Nottingham effect and for the value of the inversion temperature for tungsten. The purpose of the present work was to permit a better check of existing theory through careful measurement of the Nottingham effect for both clean and coated tungsten field emitters.

II. EXPERIMENTAL APPROACHES

The main difficulty in measuring energy-exchange phenomena in field and T-F emission is the strong localization of these phenomena and of the associated temperature changes; this localization results from the cathode geometry (very sharp needles with a conical shank and a tip radius well below 1 μ) with which controlled field emission is most reliably obtained. A determination of both the magnitude and the location of the energy transfer requires measurement of the temperature at the emitting area itself, which is of the order of 10^{-9} cm^2. For this purpose, temperature-sensitive coatings of materials which alter the cathode work function can be used to sense the local tip temperature. Measurements of this type, discussed in this paper, conclusively established the existence of emission heating and cooling domains; within limit of experimental accuracy, they also confirm the magnitude of the energy exchange and its localization within a few tip radii of the cathode tip. However, the complex experimental conditions (pulsed emission, large field, and temperature gradients near the tip, etc.) limit the accuracy of this approach; therefore, a more precise method has been used to measure the magnitude (but not the location) of the energy exchange and the inversion temperature, i.e., the temperature for which $\langle E \rangle = \langle E' \rangle$.

A. Temperature-Sensitive Coatings

One method of estimating the local temperature at the emitter tip consists of coating the emitter with adsorbates whose desorption or surface-migration temperatures are determined in a separate experiment. We have employed this method primarily to establish the degree of localization of the energy-exchange process and to obtain a qualitative estimate of the emitter-tip temperature. The main difficulty in employing this method for quantitative temperature determination during emission arises from field effects[13] on the thermal-desorption and surface-migration rates.

The method employed by us consisted of depositing cesium, barium, or zirconium co-adsorbed with oxygen onto a tungsten emitter at low temperature in a standard field electron microscope tube. After migrating the adsorbate across the emitter by heating, the emitter was cooled and a 1-μsec square-wave pulsed voltage (at a repetition rate of 100 pulses/sec) was applied to the anode in order to draw a field emission current sufficient to heat the emitter tip. The high emission current (approximately 30 to 100 mA) necessary to cause an appreciable temperature change, restricted the experiment to low-duty-factor pulsed emission since dc emission currents of such high levels will usually cause severe instability of the emission.

From the adsorbate coverage change after a specified emission time (as determined from work-function variation) due to thermal desorption, the maximum temperature of the emitter could be inferred from previous thermal-desorption data. Field electron emission patterns were also analyzed in order to ascertain the regions of the emitter which exhibited adsorbate removal.

B. Direct Measurement of the Energy Exchange

The method employed to obtain quantitative measurement of the energy exchange accompanying field emission is a refinement of that used by Drechsler,[12] who obtained field and T-F emission from random protrusions on the surface of very thin wires. Briefly stated, the method is to provide an emitter support filament of sufficient thermal impedance that the small heat input resulting from a low-field electron-emission current may be detected sensitively through the associated change in temperature and resistance of the filament. Reliance on emission from several random protrusions of unknown number, geometry, and location creates uncertainties in the interpretation of the data which are avoided here by confining emission to a single field-emission needle (whose precise geometry could be determined in an electron microscope and from field electron emission I-V characteristics) mounted at the center of a smooth wire 1-in. long and approxi-

[8] F. M. Charbonnier, Wright Air Development Division Technical Report No. 59-20(AD-272760), 1960 (unpublished).
[9] F. M. Charbonnier, in Ninth Field Emission Symposium, Notre Dame University, 1962 (unpublished).
[10] P. H. Levine, J. Appl. Phys. 33, 582 (1962).
[11] M. Drechsler, in Eighth Field Emission Symposium, Williams College, 1961 (unpublished); Tenth Field Emission Symposium, Berea College, 1963 (unpublished).
[12] M. Drechsler, Z. Naturforsch. 18a, 1376 (1963).
[13] L. W. Swanson, R. W. Strayer, and F. M. Charbonnier, Surface Sci. 2, 177 (1964).

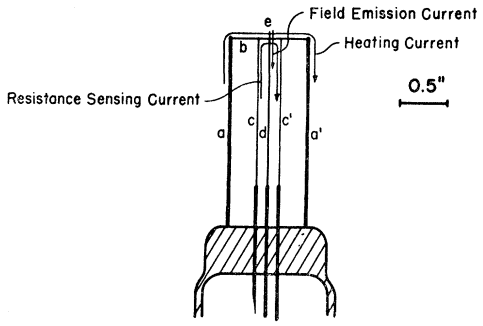

FIG. 1. Diagram of tip assembly used in tube for studying emission heating and cooling. Field emitter is formed at end of central lead.

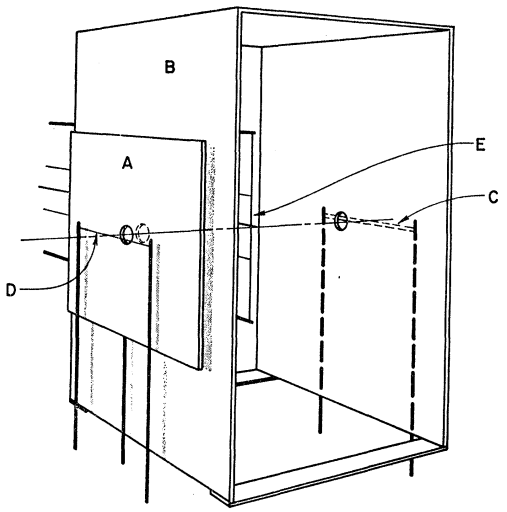

FIG. 2. Diagram showing tip assembly, associated filaments, and electrodes for quantitative study of emission heating and cooling.

mately 1.1 mil in diameter. The tip assembly shown in Fig. 1 consists of two 40-mil molybdenum rods a and a' supporting the emitter support wire b to which two 0.5-mil potential leads c and c' are spot welded for sampling resistance changes across a 200-mil portion of the emitter support filament. The central 1.1-mil diam lead d carried the emission current in order to eliminate any IR drops on the emitter-support filament due to the emission current itself. The temperature of the emitter e was controlled by adjusting a dc heating current through the filament b; the temperature was derived, to an accuracy of approximately 3%, from the resistance R of the 200-mil section of the emitter-support filament. The thermal impedance of the structure was sufficiently large that emission-induced power inputs as low as 10 μW could be detected and measured. This had the advantage of permitting good measurements to be made at low dc current levels where the emission is highly stable and where the Nottingham effect strongly predominates, resistive heating (which can be calculated only approximately) having only a relatively small effect. The emission-induced power input H at the emitter was derived from the change ΔR in support-filament resistance caused by the associated change ΔT in support-filament temperature. The experiment was confined to power inputs H small enough that ΔT and hence, ΔR could be considered proportional to H. The experiment depended on the reliable determination of $c_0=\Delta R/H$ as a function of emitter temperature. This was extremely difficult to calculate because of the complex geometry of the emitter assembly and the importance of radiation losses at high temperatures. Hence, the tube was designed to permit direct experimental calibration of ΔR in terms of a known power input H. For this purpose the emitter could be bombarded by a fine 30-mil×5-mil electron sheet beam generated by an auxiliary filament, D of Fig. 2, and focused by an 800-G magnetic field at the cathode tip; ΔR was measured as a function of bombarding-beam power at various cathode temperatures. Alignment of the electron beam, so that it impinged on as small a section as possible of the 20-mil-length field emitter, was accomplished by first aligning the emitter structure during fabrication so that only the very tip of the emitter protruded through the 30-mil circle defined by the aperture on plate A. The direction of the magnetic field was then adjusted during operation, while simultaneously measuring the beam current striking the emitter and the wire filaments C. The latter consisted of two 10-mil zirconium wires separated by 5 mils and served a two-fold purpose: (1) to determine the proper alignment and distribution of the bombarding beam during the emitter calibration, and (2) to serve as a source of zirconium which could be deposited onto the emitter for the purpose of changing the work function of the tip during the study of the Nottingham effect.

The actual power calibration of the emitter assembly was performed by measuring ΔR versus the known power input H_b at the emitter due to the bombardment current I_b at various emitter temperatures ranging from 300 to 1100°K. For each temperature, a straight line was obtained and its slope yielded the value of c_0 (as shown in Fig. 3) as a function of temperature. As expected, c_0 increased at low temperatures (as the thermal conductivity of tungsten decreases) then decreased at high temperatures as radiation losses became predominant. During the experimental measurements of ΔR versus H_b the potentials of the various tube elements were as follows: $V_D=-222$ V, $V_A=0$, $V_B=-200$ V, $V_E=0$ V, and $V_C=0$ V. This prevented secondary emission from the emitter and insured that the only secondary electrons able to reach the emitter had originated at plate B and therefore possessed nearly full voltage. Furthermore, with careful beam alignment the number of such secondaries was very small since the beam was collimated by aperture A to a diameter much smaller than that of the apertures on B. Hence, H_b could without

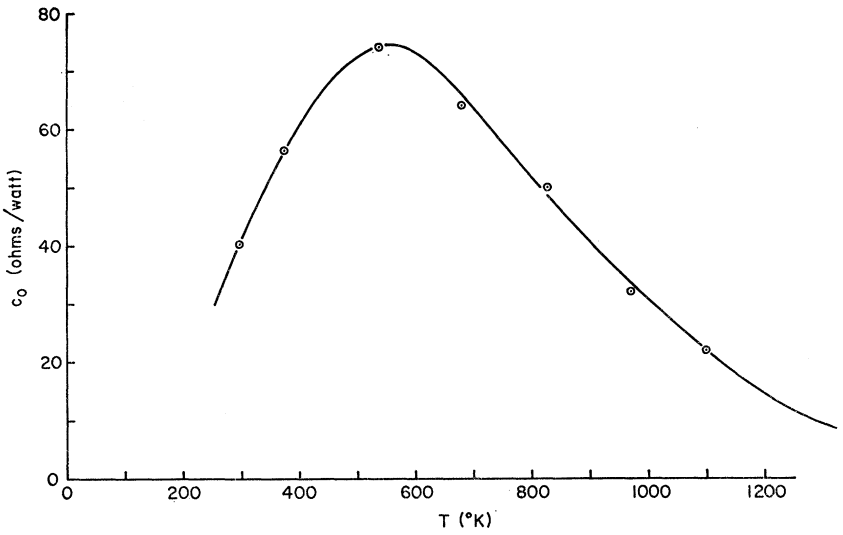

FIG. 3. Plot of experimentally determined conversion factor (for converting ΔR changes to H) as a function of emitter temperature.

significant error be approximated by the product of V_D and the total current collected at the emitter.

The tube envelope was made of alumino-silicate glass in order to minimize helium diffusion in the tube after seal off. The tube embodiment was such that field electron patterns from the emitter could be displayed on a fluorescent screen in order to ascertain the orientation and cleanliness of the emitter surface. Tip cleaning was accomplished by a combination of electron bombardment and resistive heating of the emitter. The pressure was sufficiently low that, at low emission levels, contamination of the emitter surface remained negligible several hours after initial cleaning.

During the investigation of emission heating, field electron currents up to 500 μA were drawn from the emitter. In order to minimize contamination of the tip at the maximum current level, a magnetic field was applied in a direction such that the emitted current was collected on the anode plates B of Fig. 2, which had previously been well outgassed by electron bombardment during the tube evacuation and could therefore dissipate appreciable power without significant release of contaminants.

Resistivity changes developed across the emitter-support filament, due to emitter temperature variations caused by either emission heating or electron bombardment during calibration, were measured by a Keithley Model 660 differential voltmeter which was capable of measuring voltage changes due to ΔR with a precision of approximately 1 part in 5000. The current passing through the emitter-support filament was adjusted to the value necessary to give the required tip temperature (as determined by a previous calibration curve of filament resistance versus temperature) and was also measured by monitoring the voltage drop across a standard 1-Ω resistor through which the filament current flowed.

III. THEORETICAL CONSIDERATIONS

A theoretical expression for the energy exchange between the field-emitted electron current and the lattice is necessary for comparison with experimental results. Although such a calculation, based on a free-electron model, was previously published by Levine,[10] it will be instructive to consider the structure of the calculation in order to delineate clearly the limitations and applicability of the model and the resulting analytical expressions.

We consider first a cathode field emitting electrons with an average electron energy $\langle E\rangle$, which are collected at the anode and subsequently conducted back to the cathode through a conductor at temperature T. Letting $\langle E'\rangle$ be the average energy of the conduction electrons in the emitter, then a net energy exchange of an amount

$$\epsilon_N=\langle E\rangle-\langle E'\rangle \tag{1}$$

is released to the lattice at the cathode. As pointed out originally by Nottingham,[5] for the case $T=0$ conduction in the external circuit occurs at the Fermi level (except through the batteries) and

$$\epsilon_N=\langle E\rangle-E_f^0, \tag{2}$$

where E_f^0 is the 0°K Fermi energy. It is convenient to proceed by first deriving the expression for $\langle E\rangle$ in terms of the electric field and surface work function and then examining the variation of $\langle E'\rangle$ with temperature.

A. Average Total Energy of the Emitted Electrons

An expression for the average total energy $\langle\epsilon\rangle$ (relative to the Fermi level, i.e., $\langle\epsilon\rangle=\langle E\rangle-E_f$) of the field-emitted electrons can be obtained directly from the expression for the total energy distribution of field-emitted electrons. The situation is depicted in Fig. 4, which gives a one-dimensional potential plot of the surface of a

metal (Sommerfeld free-electron model assumed) with work function ϕ and externally applied field F. At $T=0°K$ all electron levels of the metal above the Fermi level E_f are empty and emitted electrons must necessarily originate from below E_f. The total energy distribution depicted in Fig. 4 is an exponential curve with maximum at E_f for $T=0°K$, which then changes shape and becomes symmetrical about E_f at a certain temperature T^*, which depends on field and work function. $\langle\epsilon\rangle$ is negative below T^* and positive above T^*.

An expression for the current density per unit total energy (relative to E_f) $J(\epsilon)$ was derived recently by Stratton[14] for a degenerate metal of arbitrary band structure. This can be written as

$$J(\epsilon)=\frac{2ef(\epsilon)}{h^3}\int\int D(E-E_\perp)dp_y dp_z, \tag{3}$$

where $f(\epsilon)$ is the electron distribution function and

$$E_\perp=(p_y^2+p_z^2)/2m \tag{4}$$

is the energy transverse to the emission direction. The integration over the transverse momenta must be carried over all values of p_y and p_z which, for a particular constant-energy surface ϵ, are inside the shadow of the energy surface projected on a plane perpendicular to the emission direction. Assuming specular transmission (i.e., no discontinuity in $E_\perp$ at the emitting surface), the WKB approximation for the transmission coefficient is

$$D(E_x)=e^{-B(E_x)}. \tag{5}$$

Expanding the exponential in a Taylor series about E_f, one obtains $D(E_x)$ in the well-known form

$$D(E_x)\cong e^{-b+(E_x-E_f)/d-\cdots}, \tag{6}$$

where

$$b=\frac{4}{3}\frac{(2m\phi^3)^{1/2}}{\hbar eF}v(y)=6.83\times10^7\phi^{3/2}v(y)/F \tag{7}$$

and

$$d=\frac{\hbar eF}{2(2m\phi)^{1/2}t(y)}=\frac{9.76\times10^{-9}F}{\phi^{1/2}t(y)}(\text{eV}) \tag{8}$$

if F is in V/cm and ϕ in eV. The correction terms $t(y)$ and $v(y)$, which are due to the image potential, are tabulated[15] slowly varying functions of the auxiliary variable $y=(e^3F)^{1/2}/\phi$. Combining Eqs. (3) and (6), retaining only the first two terms in the exponential of Eq. (6), introducing polar coordinates $E_\perp$ and ϕ_p, and integrating $E_\perp$ from 0 to E_m leads to the following form of the total energy distribution $J(\epsilon)$ of the emitted current density:

$$J(\epsilon)=\frac{J_0 f(\epsilon)e^{\epsilon/d}}{d}\left[1-\frac{1}{2\pi}\int_0^{2\pi}e^{-E_m/d}d\phi_p\right], \tag{9}$$

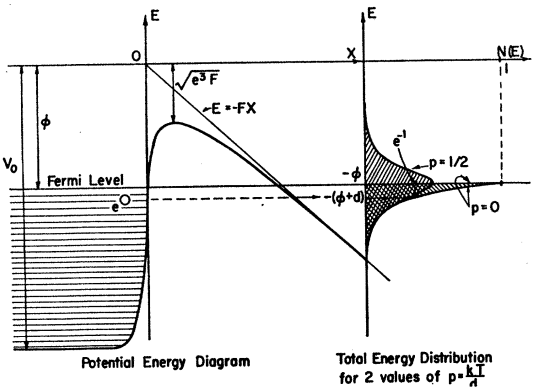

FIG. 4. Potential-energy diagram and total energy distribution for field and T-F emitted electrons.

where J_0 denotes the total current density (integrated over all energies) at 0°K, which is given by

$$J_0=\frac{e^3F^2}{8\pi\phi t^2(y)}e^{-b}=\frac{1.54\times10^{-6}F^2}{\phi t^2(y)}\times e^{-6.83\times10^7\phi^{3/2}v(y)/F}(\text{A/cm}^2), \tag{10}$$

and where E_m is the maximum value of $E_\perp$ for a specified energy surface ϵ and polar angle ϕ_p in the yz plane. The specific effect of band structure occurs only through the integral of Eq. (9) and can be neglected when $E_m/d\gg1$. Under normal field-electron-emission conditions $d\cong0.15$ to 0.25 eV, and it is reasonable to believe that E_m is sufficiently large so that, for most degenerate metals exhibiting large Fermi energies, band-structure effects are negligible; however, for transition metals with partially filled narrow d bands, Fermi-surface shapes along certain crystallographic directions may be sufficiently small to perturb $J(\epsilon)$ through the band-structure term. This possibility and its experimental observation for the case of tungsten are discussed in a recent paper.[16]

Neglecting band-structure effects and inserting the Fermi-Dirac distribution $f(\epsilon)$ into Eq. (9) gives

$$J(\epsilon)=\frac{J_0}{d}\left[\frac{e^{\epsilon/d}}{1+e^{\epsilon/pd}}\right], \tag{11}$$

where $p=kT/d$ is a dimensionless parameter. The mathematical derivation of Eq. (11) breaks down for $p\gtrsim1$ and becomes unreliable when p exceeds about 0.7. Equation (11) is identical to the original derivation of $J(\epsilon)$ by Young[17] based on the Sommerfeld free-electron model and is plotted in Fig. 4 for $p=0$ and $p=0.5$. The latter value of p has an exactly symmetrical distribution of the emitted electrons about E_f, and leads to $\langle\epsilon\rangle=0$. This condition, $p=\frac{1}{2}$, provides a simple expression for

[14] R. Stratton, Phys. Rev. **135**, A794 (1964).
[15] R. H. Good and E. W. Müller, *Handbuch der Physik*, edited by S. Flügge (Springer-Verlag, Berlin, 1956), Vol. 21, p. 176.
[16] L. W. Swanson and L. C. Crouser, Phys. Rev. Letters **16**, 389 (1966).
[17] R. D. Young, Phys. Rev. **113**, 110 (1959).

the "inversion temperature":

$$T^*=\frac{d}{2k}=\frac{5.67\times10^{-5}F}{\phi^{1/2}t(y)}(°\mathrm{K}). \quad (12)$$

If, as suggested in the introductory remarks, the average energy of the conduction carriers is near E_f, no net energy exchange occurs at T^*, and the significance of T^* is that it separates emission heating (for $T<T^*$) and cooling (for $T>T^*$).

The integration of Eq. (11) over ϵ leads to the well-known expression for the current density J_{TF}:

$$J_{TF}=J_0\int_{-\infty}^{\infty}e^{\epsilon/d}[1+e^{\epsilon/pd}]^{-1}\frac{d\epsilon}{d}=J_0\frac{\pi p}{\sin\pi p}, \quad (13)$$

which holds almost exactly in the region $0\geqslant p>0.7$. Using the lower limit of $-\infty$ in place of the correct value of $-E_f$ in order to facilitate integration does not greatly alter the result because of the exponential decrease of $J(\epsilon)$ for $\epsilon<0$. For small values of p (i.e., low T or high F), $\pi p/\sin\pi p\cong1$ and the 0°K approximation of the Fowler-Nordheim equation $J=J_0$ is obtained as given in Eq. (10).

An analytical expression for $\langle\epsilon\rangle$ can be obtained from Eq. (1) by performing the following integration:

$$\langle\epsilon\rangle=\int_{-\infty}^{\infty}\epsilon J(\epsilon)d\epsilon\Big/\int_{-\infty}^{\infty}J(\epsilon)d\epsilon=-df(p). \quad (14)$$

For the cases depicted in Fig. 4 the function $f(p)$ is unity for $p=0$ and zero for $p=0.5$; thus, for field-emitted electrons at $T=0$, $\langle\epsilon\rangle=-d$, and at $T=T^*$, $\langle\epsilon\rangle=0$. Levine[10] has shown that $f(p)\cong\pi p/\tan\pi p$, so that Eq. (14) may be written in an alternative form

$$\langle\epsilon\rangle=-\pi pd\cot\pi p. \quad (15)$$

The form of Eq. (15) predicts $\langle\epsilon\rangle/d$ to be a function of p only, as shown graphically in Fig. 5. In order to obtain simple and useful analytical expressions for $\langle\epsilon\rangle$ and T^* [Eqs. (12) and (15)], the foregoing derivation uses some customary approximations, particularly the limitation of the tunneling probability $D(E_x)$ to the first two terms of a series expansion [see Eq. (6)]. Using computer techniques, this approximation can be avoided and more precise numerical values can be obtained. In a recent computer calculation for tungsten, Brodie[18] reported values approximately 30% higher for the inversion temperature, attributing the difference to the approximation in $D(E_x)$ used to derive Eqs. (12) and (15) above. Further study shows that Brodie erroneously used the normal energy distribution of the field-emitted electrons and obtained a faulty inversion temperature T_n^* by requiring that the average *normal* energy $\langle E_n\rangle$ be equal to the Fermi energy. This is not the case since the field-emitted electrons carry a substantial average transverse energy and the inversion temperature (no energy exchange) occurs when the average *total* energy of the emitted electrons is equal to the Fermi energy, the average normal energy being then substantially smaller.

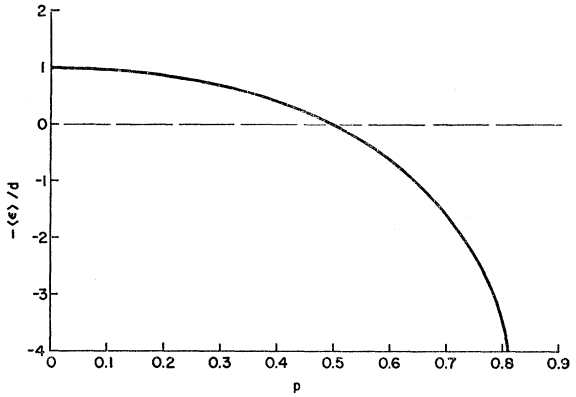

FIG. 5. A plot of $-\langle\epsilon\rangle/d$ versus p according to Eq. (15).

An approximate expression for the average normal energy $\langle\epsilon_n\rangle=\langle E_n\rangle-E_f$ is readily obtained with our model, yielding

$$\langle\epsilon_n\rangle\cong-d[1+f(p)]=-d[1+\pi p\cot\pi p]. \quad (16)$$

Brodie's temperature T_n^* corresponds to $\langle\epsilon_n\rangle=0$; therefore $f(p)=-1$ and $p=0.65$ in view of Fig. 5. This can be contrasted with the conditions $f(p)=0$ and $p=0.50$ for $\langle\epsilon\rangle=0$. Since $p=kT/d$ is directly proportional to temperature, it follows that

$$T_n^*/T^*=0.65/0.50=1.3, \quad (17)$$

which accounts for the difference between Brodie's values and those predicted by Eq. (12). Recently corrected computer calculations by Lee and Alpert,[19] yet unpublished, confirm that, when p approaches unity the approximation for $D(E_x)$ breaks down. Also Eqs. (12) and (15) are essentially correct and negligible error is made up to $p=0.7$ by omitting the quadratic and higher order terms in Eq. (6) for $D(E_x)$.

Though the average normal and total energy increase with field emitter temperature, comparison of Eqs. (15) and (16) shows that the average transverse energy of the field emitted electrons is equal to d and independent of temperature, at least within the range of validity of the foregoing calculations.

B. Average Energy of the Conduction Electrons

For a Fermi gas at temperature T, conduction involves only those electron states for which the derivative of the Fermi function $df(E)/dE$ is finite. Since the derivative of the Fermi function is appreciable only in a range of a few kT about E_f, it is clear that conduction is limited to states near the Fermi surface at low temperatures. In our experiments, the values of kT ranged

[18] I. Brodie, Intern. J. Electron. 18, 223 (1965).
[19] D. Alpert and D. A. Lee (private communication).

from 0.02 to 0.07 eV, while experimental values of ϵ_N ranged from -0.60 to $+0.30$ eV; hence, near the inversion condition ($\epsilon_N=0$) a variation of $\langle E'\rangle$ by a few hundredths of an eV may cause the inversion temperature to depart significantly from the predicted value based on Nottingham's assumption that $\langle E'\rangle=E_f$. It is therefore instructive to obtain the expression for the average energy of the charge carriers in a conductor possessing a temperature gradient and internal electric field.

An expression for $\langle E'\rangle$ has been given by Mott and Jones[20] for a conductor in which the electron energy E is an arbitrary function of the wave vector k. A slightly different expression for $\langle E'\rangle$ has been derived by Seitz[21] by considering the Sommerfeld-Lorentz solution of the Boltzmann transport equation. In the latter case the interaction of the electrons (viewed as a degenerate Fermi gas) with the lattice is contained in a function $\lambda(E,T)$ representing the mean free path of the conducting electrons. The final form of the expression to the first order in kT/E_f is

$$\langle E'\rangle\cong E_f+\frac{(\pi kT)^2}{3}\left[\frac{1}{E_f}+\frac{\lambda'(E_f,T)}{\lambda(E_f,T)}\right], \tag{18}$$

where $\lambda'(E_f,T)$ is the value of the first derivative of λ with respect to E at the Fermi level. The function $\lambda(E_f,T)$ is undetermined by the Sommerfeld-Lorentz theory and must be calculated from more detailed quantum-mechanical approaches. The direction and magnitude of the variation of $\langle E'\rangle$ with T is ultimately governed by the function $\lambda(E_f,T)$.

Upon examining the expectation regarding the direction of the variation of $\langle E'\rangle$ with T for a more general model, Mott and Jones[20] concluded that $d\langle E'\rangle/dT$ should be positive for metals possessing partially filled bands and negative for those possessing nearly filled bands. They further concluded that transition metals with overlapping s and d bands, in which the main resistance producing factor is $s\rightarrow d$ transitions, should exhibit a positive $d\langle E'\rangle/dT$ for a nearly filled d band, whereas for a partially filled d band the sign of $d\langle E'\rangle/dT$ will depend on the $E(k)$ and $\lambda(E,T)$ relationships near the top of the Fermi distribution. As expected, both positive and negative $d\langle E'\rangle/dT$ have been measured for the transition metals and, for many, both the magnitude and sign of $d\langle E'\rangle/dT$ vary with temperature.

In view of the limited knowledge of the $E(k)$ and $\lambda(E,T)$ relationships for most transition metals, it is more fruitful to estimate the variation of $\langle E'\rangle$ with T from experimental values of $\langle E'\rangle$ versus T rather than from first principles through Eq. (18). This can be accomplished as pointed out by Seitz,[21] by expressing $\langle E'\rangle$ in terms of the thermoelectric power S as follows:

$$\langle E'\rangle=E_f-eTS, \tag{19}$$

where

$$S=\int_0^T\frac{\mu}{T}dT \tag{20}$$

and μ is the Thompson coefficient of the metal. The quantity eTS represents the reversible heat carried by the current whose direction of flow, relative to the current flow and temperature gradient, depends on the sign of μ. In keeping with the usual convention a positive μ signifies the evolution of heat as electrons go to places of higher temperature and according to Eq. (19), a lowering of the average energy of the charge carriers.

Based on Potter's[22] values of S for tungsten, one finds that $\langle E'\rangle-E_f$ varies with T as shown in curve (a) of Fig. 6. On this basis one can expect a small decrease in $\langle E'\rangle-E_f$ with increasing temperature (e.g., 0.015 eV at 900°K).

C. Emitter Temperature

Both Nottingham and Joule heating must be considered in determining the temperature change produced by the energy-exchange processes accompanying field-electron emission. In the case of the Nottingham effect, the energy exchange between the conduction electrons and the lattice is expected to occur within a fraction of an emitter-tip diameter (approximately 10^{-5} cm) in view of the extremely short mean free path of conduction electrons near the Fermi energy with respect to electron-phonon and electron-electron interactions. The details of the energy exchange between those electrons taking part in the conduction current and those

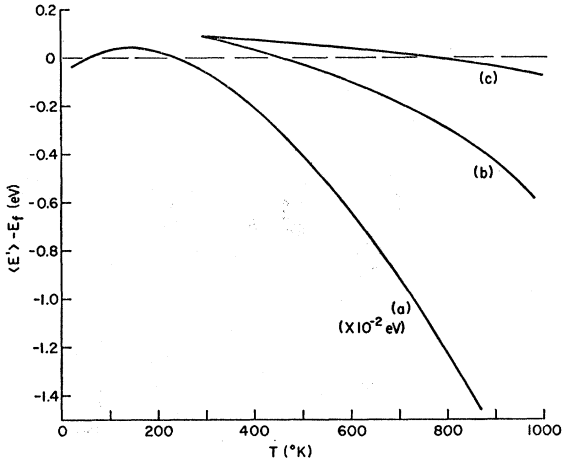

FIG. 6. Curve (a) shows the expected variation of $\langle E'\rangle-E_f$ according to Eq. (19) and based on Potter's (Ref. 22) thermoelectric data for tungsten. Curves (b) and (c) give the predicted variation of $\langle E'\rangle-E_f$ based on a comparison between the experimental and theoretical results of Fig. 13 at $F=6.0$ and 5.0×10^7 V/cm, respectively.

[20] N. F. Mott and E. H. Jones, *The Theory of the Properties of Metals and Alloys* (Oxford University Press, London, 1936), pp. 305–314.

[21] F. Seitz, *Theory of Solids* (McGraw-Hill Book Company, Inc., New York, 1940), p. 179.

[22] H. H. Potter, Proc. Phys. Soc. (London) **53**, 695 (1941).

taking part in the emission current is a matter which requires further theoretical studies; its calculation is obviously more complex for nonfree-electron metals where the functional dependence of $\langle E' \rangle$ on temperature may differ appreciably from a simple free-electron model.

Assuming for the remaining part of this discussion that the Nottingham energy exchange with the lattice is $\epsilon_N = \langle \epsilon \rangle$, i.e., that $\langle E' \rangle = E_f$, then one obtains for the total power input H to the lattice

$$H = \langle \epsilon \rangle I_e + H_r, \tag{21}$$

where I_e is the total emitted current. H_r is the power input due to Joule heating, and positive values of H refer to a net power input to the lattice.

Next, we consider the energy input due to the Joule heating term H_r. An approximate expression for the resistive power exchange for a conical emitter of radius r and cone half-angle α is given by the following expression:

$$H_r \cong \rho(T) I_e^2 / \pi \alpha r, \tag{22}$$

where $\rho(T)$ is the bulk resistivity at the temperature T. The complete expression for H obtained from Eqs. (15), (21), and (22) is

$$H = \pi k T I_e \cot \pi p + \rho(T) I_e^2 / \pi \alpha r. \tag{23}$$

An analytical expression for the temperature T_0 at the emitter apex compared to the temperature T_1 at the emitter base (assumed fixed) can be obtained[8] for a truncated conically shaped emitter of radius r_0 at the point of truncation; neglecting radiation losses and assuming $r_0 = r$, the expression takes the form

$$T_0 - T_1 = \frac{kT \cot \pi p}{K} \left(\frac{I_e}{\alpha r} \right) + \frac{\rho(T)}{2K\pi^2} \left(\frac{I_e}{\alpha r} \right)^2, \tag{24}$$

where K is the thermal conductivity. The first term in Eq. (24) is due to the Nottingham effect, whereas the second term is caused by Joule heating. It has been found by Houston[23] that approximately the same value of T_0 is obtained for a conical emitter if one considers the variable resistivity at various points or if one uses for simplicity a constant value of $\rho(T)$ corresponding to an "effective" temperature $T = 0.8T_0$, i.e., $\rho(T) = \rho(0.8T_0)$. The neglect of radiation losses means the emitter tip is slightly cooler than that calculated by Eq. (24), but in the case of emitter sizes utilized in this study the radiative correction to the tip temperature is less than 0.5% at 1000°K and therefore can be neglected.

IV. RESULTS

A. Temperature-Sensitive Coatings

As mentioned previously, the observed temperature stability of field emitters at high current-density levels, where Joule heating by itself should cause strong instability, provided initial evidence of the Nottingham effect. It was subsequently observed that strongly bound adsorbed layers on tungsten, such as zirconium-oxygen layers, which lowered the work function, also reduced the emitter temperature and allowed even greater emitted current densities before the onset of excessive tip heating. In one experiment, illustrated in the photos of Fig. 7, a peak pulse current (duty factor approximately 10^{-4}) of 57mA was obtained from a clean, ⟨110⟩ oriented tungsten emitter before the onset of instabilities due to Joule heating. This current caused sufficient heating to activate diffusion phenomena, producing slip planes, and roughening of the tungsten surface. After annealing the emitter to restore a smooth surface and applying a zirconium coating to the emitter, a pulse emission current of greater than 102 mA was obtained. This results from the increased emission cooling characteristics of the lower work-function ($\phi = 2.8$ eV) surface. Thus, the tip temperature was substantially less than for the clean emitter at half the current. As shown in Fig. 7(c), the lowering of the work function due to zirconium adsorption occurs selectively in the {100} regions, while the remaining surface exhibits

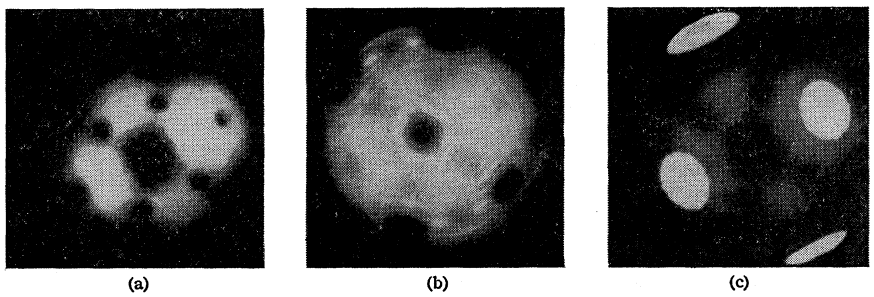

(a) (b) (c)

FIG. 7. (a) Typical field electron pattern of clean and smooth ⟨110⟩ oriented tungsten emitter. (b) Pattern of the same emitter, showing cumulative disruption of the clean tungsten surface (just prior to vacuum arc) resulting from emission of a peak pulse current of 57 mA at 15.3 kV ($\phi = 4.52$ eV) with a duty factor of 10^{-4}. (c) Pattern of the same emitter, with an adsorbed zirconium-oxygen layer and emitting stably a peak pulse current of 102mA at 14.8kV ($\phi = 2.8$ eV for the brightly emitting areas).

[23] J. Houston (private communication).

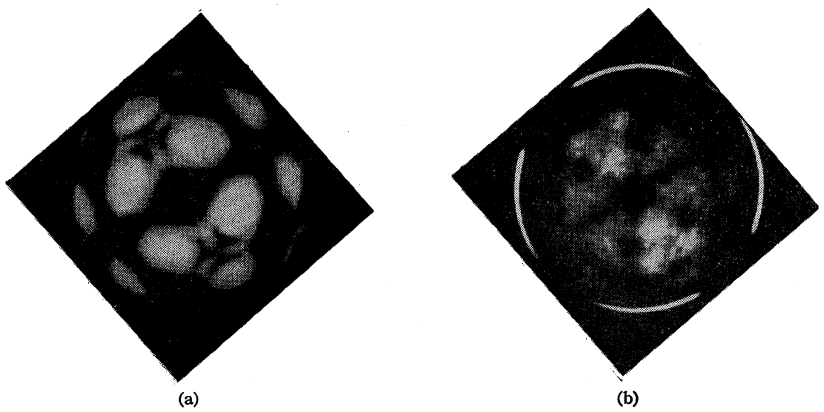

FIG. 8. (a) Pulse field electron pattern of a near monolayer coverage of barium on tungsten exhibiting an average work function of 2.0 eV. Picture taken at 3.4 kV. (b) Same as pattern (a) but after emitting 84 mA of peak pulse electron current at a duty factor of 10^{-4} for 300 sec. Picture taken at 7.8 kV.

nearly clean tungsten characteristics and the emitted current density in the zirconium-coated regions of pattern 7(c) is approximately 4 times that of the clean tungsten surface in pattern 7(b).

These observations are consistent with the foregoing theory of the Nottingham effect. Equation (10) shows that a constant current density J requires

$$\phi^{3/2}/F \cong \text{const} = C. \tag{25}$$

Combining Eqs. (25) and (12) gives the following expression for the inversion temperature at a constant J:

$$T^* \cong (5.67 \times 10^{-5}\phi)/t(y)C \tag{26}$$

for ϕ in eV. Thus, a lower T^* (or larger cooling effect) is obtained at a constant J as ϕ decreases, the inversion temperature being roughly proportional to work function. Alternatively, for a given allowed tip temperature a larger J can be obtained as ϕ decreases.

From the behavior of other adsorbates a qualitative estimate of the magnitude and location of the heating effects was obtained. Figure 8(a) shows the pulse field electron pattern of a tungsten emitter with near monolayer coverage of barium sufficient to cause a lowering of the work function from 4.5 to 2.0 eV; Fig. 8(b) shows the same pattern after emitting a pulse field electron peak current (duty factor about 10^{-4}) of approximately 80 mA for 300 sec. The pattern shows a large decrease in barium coverage at the tip, to only a few tenths monolayer, due to emission-induced heating and consequent evaporation of barium. However, the bright ring surrounding the pattern shows that barium was removed only from the very tip of the emitter, indicating that emission heating is highly localized. From an estimate of the work function in the interior of the pattern in Fig. 8(b) and knowledge of the decrease in field with increasing angle from the emitter apex, one can estimate that barium was removed back from the apex an angular distance of $\sim 120°$, which is only about twice the angular distance of the electron-emitting area in the pattern in Fig. 8(a).

Further evidence of the extreme localization of the Nottingham heating was obtained from a similar experiment using a cesium layer. Figure 9(a) shows a tungsten emitter with a cesium coverage in excess of a monolayer; Fig. 9(b) is the same surface after subjecting the emitter to a peak pulse current of 53 mA for 300 sec. The cesium coverage was reduced to approximately 0.5 monolayer coverage by thermal desorption. In contrast to the barium on tungsten sequence, no bright ring of emission was observed because of the heavier cesium coverage and lower binding energy of cesium, which caused cesium evaporation to extend further down the emitter

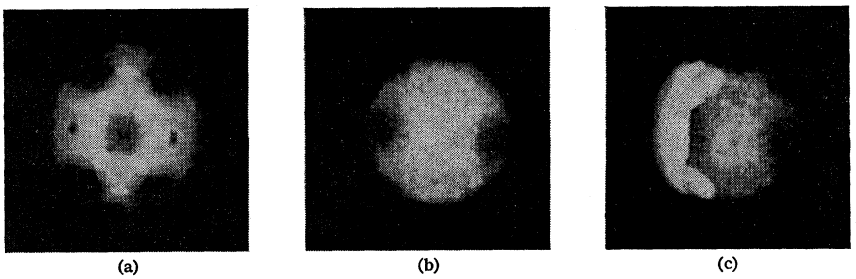

FIG. 9. (a) Pulse field electron pattern of a tungsten tip with cesium coverage in excess of one monolayer. The average work function of the covered surface is 1.78 eV. (b) Pattern of same tip but after emitting a peak pulse current of 53 mA (1 μsec pulses at 100 pps) for 300 sec; the coverage in the emitting region has decreased to approximately 0.5 monolayer, as determined by the work-function change to 2.1 eV. (c) Evidence of cesium migration from the heavily covered shank to the tip, produced by heating pattern (b) to 173°K for only 300 sec.

TABLE I. Tip temperature due to emission heating as inferred from cesium coverage change.

I_e(mA)	ϕ(eV)	ΔT_r(°K)	$\Delta T_r+\Delta T_N$(°K)	ΔT(obs)(°K)
43	1.58	18	368	338
48	1.68	26	438	347
36	2.16	12	505	743

shank. However, on heating to a temperature sufficient to cause mobility of the adsorbed cesium, a sharp boundary migrated across the tip [see Fig. 9(c)] indicating migration of the cesium from the heavily covered emitter shank to the depleted emitter tip. It could be estimated from the time and temperature required for the boundary to appear that the low-coverage cesium region extended less than a few tenths of a tip radius beyond the field of view, in general agreement with the barium results.

Using prior measurements of the temperature required to desorb cesium to various residual coverages the peak emitter-tip temperature at the end of each pulse could be estimated by methods described in Sec. II A. This experimentally determined temperature sise could then be compared with the temperature change due to both resistive ΔT_r and Nottingham heating ΔT_N, calculated according to Eq. (24). The comparison is illustrated in Table I at three different levels of emitted current. In each case the resistive heating contributes less than 6% to the total ΔT, illustrating the dominant role of Nottingham heating at low temperatures. The agreement between experiment and theory is considered satisfactory in view of the problems involved in evaluating ΔT (obs).

The investigation of the behavior of various adsorbates at very high pulsed currents has therefore established the following:

(1) Strongly bound low-work-function adsorbates (e.g., zirconium-oxygen on tungsten) allow larger current densities of emitted current than the corresponding clean substrates because of the enhanced emission cooling associated with reduced work function;

(2) Adsorbates which are thermally desorbed by emission heating provide evidence that the energy exchanges are strongly localized to an area not much greater than the emitting area;

(3) Peak tip-temperature estimates derived from the observed adsorbate removal cannot be accounted for by resistive heating alone and are in reasonable agreement with the much larger values predicted by the Nottingham-effect theory.

B. Direct Measurement of the Energy Exchange

Emission heating and cooling results were obtained on clean and zirconium-oxygen coated tungsten cathodes by emitting a specified field electron current and measuring the change in filament resistance ΔR which could, using the conversion factors given in Fig. 3, then be converted to a power exchange H at the emitter. The upper limit of emitter temperature at which such measurements could be performed was determined by the onset of field-temperature-induced deformation of the emitter tip in the case of uncoated emitters and by rearrangement of adsorbed layers in the case of zirconium-oxygen–coated emitters.

Since the measured power exchanges range from 0 to 150 μW, it is important that the field-emitted electron-beam power dissipated in the tube be as small as possible in order to eliminate ambient temperature variations. Sharp emitter tips are therefore advantageous since, at a given field-emission current, the beam voltage and power are roughly proportional to the tip radius. To minimize heating of the collector plates B of Fig. 2, measurements of ΔR at a given I_e were taken as rapidly as possible. This problem was not as serious for the low-work-function surfaces where field-emission voltages and, hence, maximum power dissipation required for a given I_e were reduced by the ratio of the work-function change to the $\frac{3}{2}$ power.

Another important experimental problem was the impingement on the emitter-support structure of high-energy ions formed at the anode. Relatively few ions can cause serious errors in the power input since the ions carry energies of hundreds to thousands of eV, as opposed to a fraction of one eV for the emitted electrons. Such ions can only be formed by electron-induced desorption processes, since temperature changes at the anode were not sufficient to cause thermal desorption of contaminants, and the tube vacuum was sufficiently good to minimize formation of ions from the residual gas. Recent investigations[24] of electron-induced desorption suggest that the number of ions formed per electron, particularly at voltages in excess of a few hundred volts, is less than 10^{-7} ions/electron; thus, an electron current of 500 μA at 4 kV should correspond to an ion power input of less than 0.2 μW, which is below the sensitivity of the measurements. It is interesting to note that an ion current as low as 10^{-13} A, though it produces negligible input power, can produce readily detected effects on the emitter surface. This was observed in the case of zirconium-oxygen-coated tungsten emitters where the field electron current at high I_e was observed to decrease rapidly as a result of erosion of the adsorbed coating by impinging ions.

1. Clean-Tungsten Results

Figure 10 shows the measured power exchange H at a clean-tungsten emitter as a function of I_e for various temperatures. The data were reproducible to within $\pm 5\%$. Similar data, taken from another tube whose emitter was blunter, were not as reproducible and gave values of H approximately 25% larger because of the larger power dissipation within the tube; how-

[24] P. A. Redhead, Can J. Phys. 42, 886 (1964).

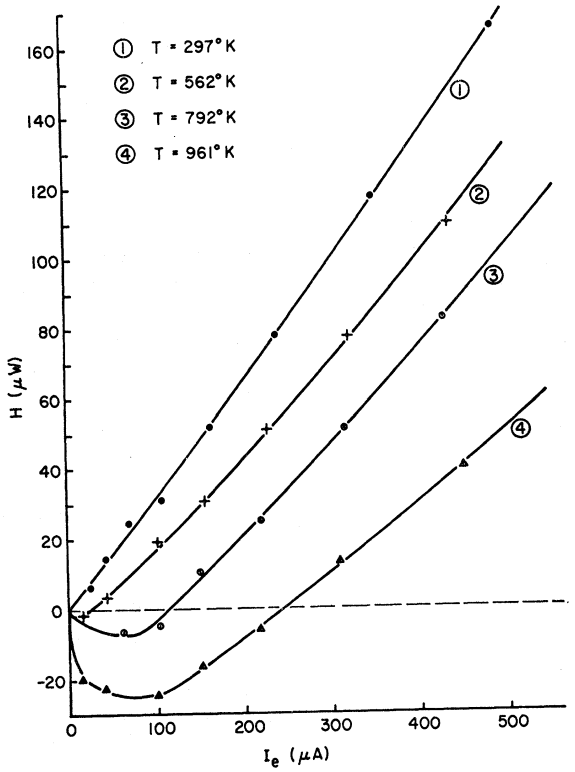

FIG. 10. Experimentally determined power exchange H at the emitter as a function of field emitted current I_e at the indicated temperatures for clean tungsten where $\phi=4.52$ eV. Negative values of H indicate emission cooling.

ever, the data confirmed the functional trends shown in Fig. 10. The field electron pattern and I_e-V characteristic were checked throughout the run to insure that contamination or geometrical rearrangement of the emitter surface remained at a negligible level.

The corrections to the emitter temperature due to the emission heating (or cooling) were small even at the highest value of I_e and could be neglected. This can be shown by rewriting Eq. (24) as follows:

$$T_0-T_1=\frac{1}{K\pi\alpha r}\left[H-\frac{H_r}{2}\right]. \tag{27}$$

For a typical emitter where $r=1.3\times10^{-5}$ cm and $\alpha=0.157$ rad, Eq. (22) gives $H_r=1.4\,\mu$W at $T=1000$°K and $I_e=600\,\mu$A. Thus, throughout the range of I_e and T investigated, H_r can be neglected. At the highest value of H investigated, e.g., $H=160\,\mu$W at $T=297$°K, Eq. (27) gives a value of 6°K for T_0-T_1, using the previously mentioned values of r and α; the maximum correction to T is therefore 2% and can be neglected, since it is comparable with the accuracy of the temperature measurement.

Three general observations can be obtained from the data given in Fig. 10:

(1) H increases nearly linearly with I_e at low temperatures;

(2) It appears that the amount of heating at a specified I_e decreases with increasing temperature;

(3) The Nottingham inversion (i.e., $H=0$) occurs at increasingly higher values of I_e (or F) as the emitter temperature increases.

The first two observations are in qualitative agreement with the predictions of Eq. (23) since the Joule heating term is negligibly small in the present experiments. Recalling that the inversion temperature T^* corresponds to $p=\frac{1}{2}$, it follows that $p=T/2T^*$ and Eq. (23) can be rewritten (neglecting the Joule heating term):

$$H\cong H_N\equiv\pi kTI_e\cot(\pi T/2T^*). \tag{28}$$

At low temperatures or large electric fields the term $\cot(\pi T/2T^*)$ is insensitive to F, thereby causing H to vary in a near linear fashion with I_e; also, as T increases the $T\cot(\pi T/2T^*)$ term decreases, thereby causing H to decrease. As T approaches T^*, H is no longer proportional to I_e, but instead depends more sensitively on the variation of T^* with F and, hence, I_e. When the condition $T=T^*$ is attained, then $H=0$. At higher temperatures Nottingham cooling is observed at low currents. However, as the emitted current is increased (at fixed emitter temperature) T^* increases according to Eq. (12) and the transition from Nottingham cooling to heating occurs at a current which increases with emitter temperature. The results of Fig. 10 are in qualitative agreement with these predictions of Eq. (12) and (28).

2. *Effect of Adsorbed Layers*

Similar results are given in Fig. 11 for a low-work-function surface consisting of a tungsten emitter coated with co-adsorbed zirconium oxygen. The extreme stability of zirconium-oxygen coatings with respect to surface migration and thermal desorption makes such coatings uniquely suited for the investigation of the Nottingham effect over a wide range of emitter temperatures. It is observed that emission cooling, i.e., $T<T^*$, occurs throughout most of the experimental temperature range except for temperatures below 550°K.

The wider occurrence of emission cooling is due to the lowering of the surface work function since, in view of Eq. (26), the inversion temperature is proportional to work function. Thus, at a given emitted current, emission cooling will begin at a lower emitter temperature and will be larger at a given temperature; conversely, greater currents can be drawn before the emitter temperature becomes excessive because of Joule heating.

V. COMPARISON WITH THEORY

The experimental results can be compared quantitatively with theory in two ways. First the inversion

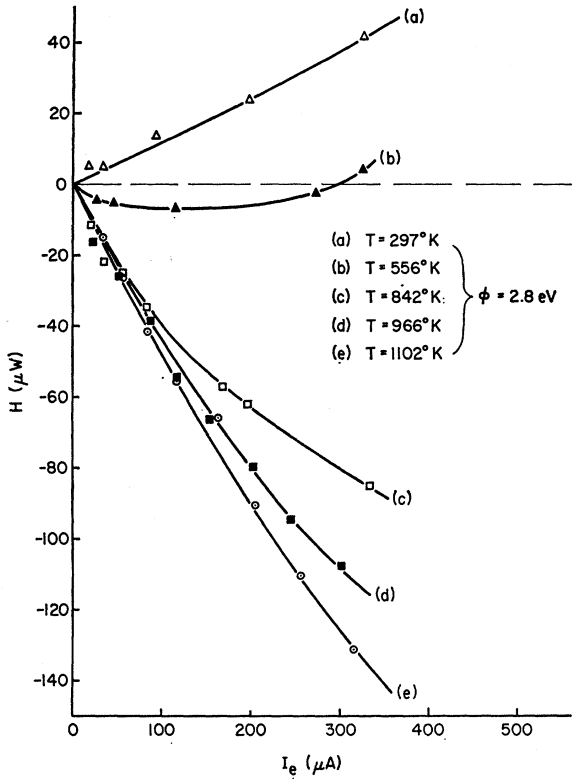

FIG. 11. Experimentally determined power exchange H at a tungsten emitter coated with zirconium-oxygen as a function of field emission current I_e. Negative values of H indicate emission cooling.

temperatures given theoretically by Eq. (12) can be compared with those obtained experimentally for clean and zirconium-oxygen-coated tungsten. Unfortunately, experimental inversion temperatures for a specified surface can only be obtained over a moderate range of emitted currents I_e and hence over a small range of fields F, since I_e is an exponential function of F. The experimental and calculated values of the inversion temperature are compared in Fig. 12 for the clean and low-work-function zirconium-oxygen-coated tungsten surfaces. In both cases the experimental inversion temperatures vary linearly with field, but are substantially below the predictions of Eq. (12). For example, at $F=4.6\times10^7$ V/cm the experimental value of T^* for clean tungsten is 550°K, as compared to the predicted value of 1165°K. Similarly, for the low-work-function zirconium-oxygen-coated surface at $F=2.4\times10^7$ V/cm the experimental value of T^* is 475°K, as compared to the predicted value of 775°K. An earlier study of the Nottingham effect by Drechsler[12] also reveals an anomalously low value of T^* for tungsten.

The above-mentioned discrepancies are significant since emission cooling of tungsten field emitters appears to occur at lower temperatures and to be much more important than predicted by the Sommerfeld model. This is further illustrated by the second method of comparing the experimental results with theory, as shown in Figs. (13) and (14) where the average energy exchange per electron ($\epsilon_N=H/I_e$), as obtained experimentally and also theoretically from Eq. (15), are plotted as a function of F. The values of F are obtained from the I_e-V characteristics plotted according to Eq. (10) in the form $\log I_e/V^2$ versus $1/V$; the slope of the latter plot yields the average value of $\beta=F/V$ provided a value for ϕ is assumed. The experimental values of ϵ_N given in Fig. 13 for clean tungsten at 297°K are larger than theory, while at higher temperatures the experimental values of ϵ_N are considerably less than expected from theory particularly at low values of F. Hence, at a fixed field ϵ_N decreases with emitter temperature much more rapidly than predicted by theory, particularly at low values of F.

Similarly, the experimental values of ϵ_N for the zirconium-oxygen-coated-tungsten results given in Fig. 14 show reasonable agreement with theory for the 297°K results, while the results above 556°K show deviations from theory similar to those noted for the clean-tungsten results. No attempt was made to calculate ϵ_N at the higher emitter temperatures (experimental curves *c*, *d*, and *e*) since the corresponding values of p exceed 0.7 and, therefore, the theory becomes seriously inaccurate. The accuracy and precision of the experimental data above 840°K, while not easily specified, is somewhat less than that of the lower temperature data because of the occurrence of some thermal-field-induced

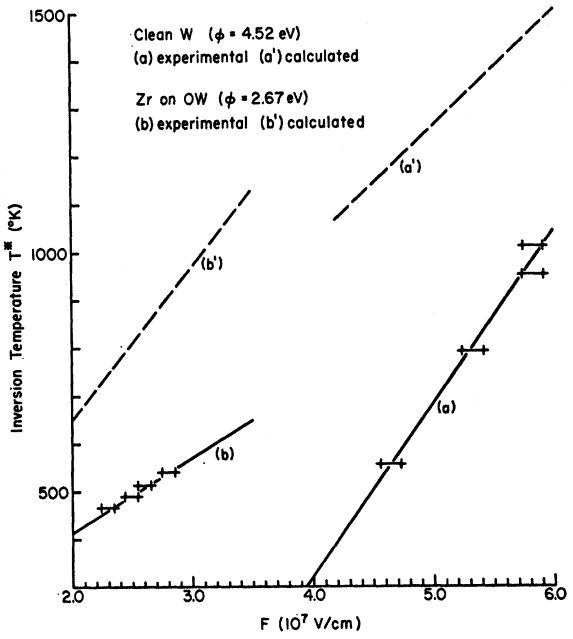

FIG. 12. Experimentally determined inversion temperatures T for a clean and zirconium-coated tungsten emitter as a function of applied electric field. Dashed curves are the respective calculated inversion temperatures according to Eq. (12).

rearrangement of the adsorbate. Nevertheless, both the clean-tungsten and zirconium-oxygen-coated-tungsten results provide clear evidence of a significant departure of the Nottingham effect from the theory based on the assumption $\langle E' \rangle \cong E_f$. As discussed in Sec. IV B, the two most likely sources of possible experimental errors are in a direction to diminish the cooling effect, and hence to further increase the observed discrepancy between experiment and theoretical expectations.

In an attempt to explain the observed anomalies in the Nottingham effect, one is led to examine the two basic premises of the theory. First: Does Eq. (11) adequately describe the total energy distribution over the temperature and field range investigated? We recall that Eq. (11) is valid for both a free-electron model and a nonfree-electron model, provided the band-structure term is negligible, i.e., $E_m/d \gg 1$. Measurements of the total energy distribution performed in the temperature range 77–300°K on tungsten have generally supported Eq. (11) and, therefore, the contemporary field-emission theory upon which Eqs. (11) and (15) are based. In order to obtain a completely rigorous check of the applicability of Eq. (11) to tungsten, it is necessary to measure the total energy distribution over a wider range of temperatures and for emission through a variety of crystal planes. These measurements, reported in preliminary fashion,[16] generally confirm the validity of Eq. (11) and yield the predicted symmetrical energy distribution at $p=0.5$, with two exceptions: The first is a markedly different shape of the energy distribution for electrons emitted along the ⟨100⟩ direction,[16] which suggests that some refinements are necessary in the basic model upon which field emission theory is based; the second is a distribution agreeing in shape but appre-

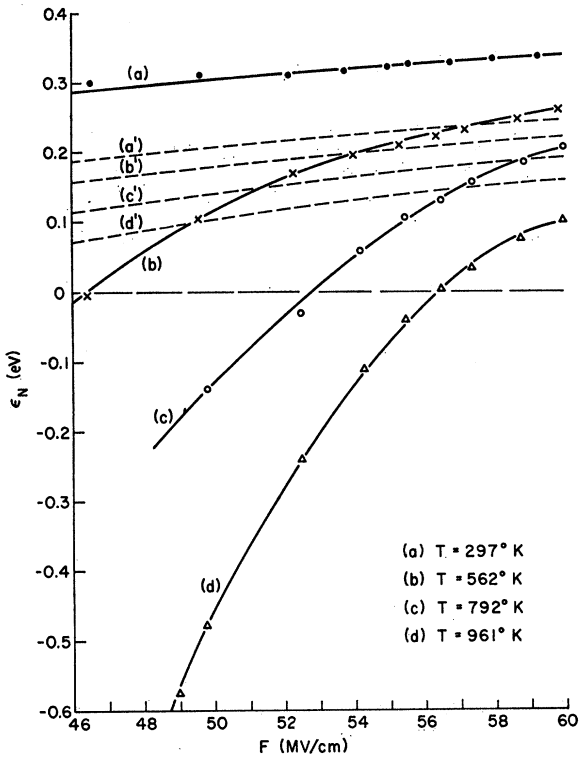

FIG. 13. Solid curves represent the experimentally determined energy exchange per electron ϵ_N with the tungsten lattice as a function of applied electric field F at the indicated temperatures for clean tungsten. Dashed curves are corresponding ones calculated according to Eq. (15). Negative values of ϵ_N indicate emission cooling.

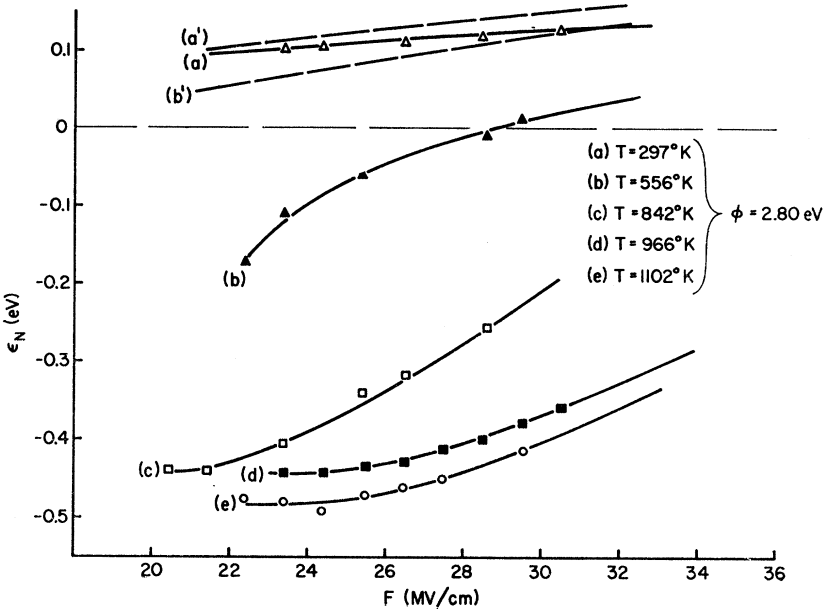

FIG. 14. Solid curves represent the experimentally determined energy exchange per electron ϵ_N with the lattice as a function of applied electric field F at the indicated temperatures for zirconium-oxygen–coated tungsten. Dashed curves are corresponding ones calculated according to Eq. (15). Negative values of ϵ_N indicate emission cooling.

ciably wider than predicted for emission in the ⟨110⟩ direction.[25]

Although measurements of the total energy distribution are not a stringent test of the free-electron nature of bulk conduction of electrons, they do provide sufficient evidence that the anomalies in the Nottingham effect cannot be attributed entirely to discrepancies in the energy distribution of the emitted electrons. This suggests an examination of the second basic premise of the Nottingham effect, namely, that the average energy of the replacement electrons is equal to the Fermi energy.

Investigations of the magneto resistance[26,27] and surface conductance[28] of tungsten have provided evidence that electrical conduction in tungsten involves nearly equal numbers of positive and negative charged carriers. If the holes of a nearly filled d band take part in the conduction, one may expect, according to the discussion following Eq. (18), a negative value of $d\langle E'\rangle/dT$. Furthermore, if the hole band possesses a low degeneracy temperature T_d, the contribution to Eq. (18) of the neglected higher order terms becomes significant as $T \rightarrow T_d$; a conduction mechanism of this nature, which causes $\langle E'\rangle$ to decrease with increasing temperature, can readily account for the anomalously low observed inversion temperatures.

A variation of $\langle E'\rangle$ with temperature should result in a uniform displacement of the experimental curves of $\epsilon_N(F)$, at various temperatures, from their theoretical values. As shown in Fig. 13, this is confirmed for the 297°K results, but the direction of the shift requires a positive $\langle E'\rangle - E_f$. In contrast, the higher temperature results of both Figs. 13 and 14 exhibit a deviation from theory which requires a value of $\langle E'\rangle - E_f$ whose magnitude and sign varies with field.

Curves (b) and (c) of Fig. 6 show the required variation in $\langle E'\rangle$-E_f necessary to account for the discrepancy between the experimental and theoretical results of Fig. 13 at $F=6.0$ and 5.0×10^7 V/cm, respectively. Although the magnitudes of the calculated curves (b) and (c) of Fig. 6 are in wide disagreement with curve (a) (based on the thermoelectric data), it is worth pointing out one interesting resemblance; that is, all three curves predict a value of $\langle E'\rangle - E_f$ whose sign varies from positive to negative as the temperature increases. While this does not provide a quantitative explanation for the disagreement with theory in the Figs. 13 and 14 results, the qualitative evidence is substantial enough to require further theoretical and experimental investigation of the connection between the thermoelectric effect and $\langle E'\rangle$-E_f. In particular, theoretical examination of bulk-conduction processes of tungsten, the mechanism of the energy exchange between the conducting charge carriers and the lattice, and the respective influence of temperature and electric field, is needed to further the understanding of the Nottingham effect.

[25] R. D. Young (private communication).
[26] E. Fawcett and W. A. Reed, Phys. Rev. **134**, A723 (1964).
[27] E. Fawcett, Phys. Rev. **128**, 154 (1962).
[28] E. Fawcett and D. Griffiths, J. Phys. Chem. Solids **23**, 1631 (1962).

VI. CONCLUSIONS

The results presented in this paper provide conclusive evidence for an energy exchange that accompanies field electron emission and which is localized to an area not appreciably greater than the emitting area of the cathode. Energy exchanges which lead to both heating and cooling of the emitter have been predicted and observed over a wide range of temperature, work function, and applied field strength. The gross trends in the variation of the energy exchange and the inversion temperature with field, temperature, and work function can be described by free-electron theory based on bulk conduction at the Fermi level. However, detailed quantitative agreement between experiment and theory is lacking, and the departures cannot be explained by experimental uncertainties. An anomalously low inversion temperature is obtained for both clean and zirconium-oxygen-coated tungsten and the values of the average energy exchange per electron is both above (at low temperatures) and below (at high temperatures) the values expected from theory.

The underlying cause of the disagreement between experiment and theory does not seem attributable to a deviation from theory in the total energy distribution of the emitted electrons, but rather to a variation of the average energy, relative to the Fermi level, of the conducting carriers with temperature and field. Further investigation of the Nottingham effect in other cathode materials which are nearly free-electron in character, and further theoretical study of the conduction processes and the electron-lattice interactions at elevated temperatures, should contribute a more detailed understanding of the Nottingham effect.

ACKNOWLEDGMENTS

The authors wish to acknowledge the support of part of this work by the National Aeronautics and Space Administration, Washington, D. C. We also wish to express our gratitude to J. K. Trolan, R. W. Strayer, and E. E. Martin for stimulating discussions and for assisting in the experimental work, and to W. P. Dyke for his interest and support.

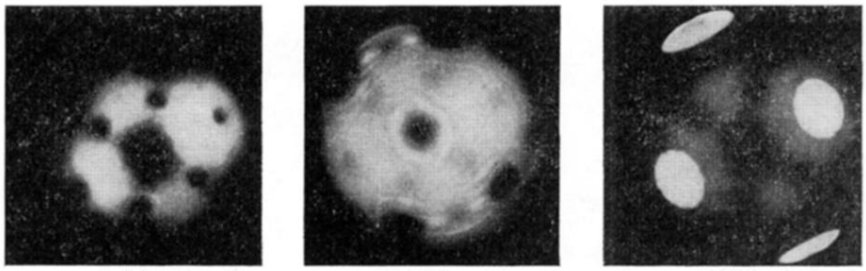

FIG. 7. (a) Typical field electron pattern of clean and smooth ⟨110⟩ oriented tungsten emitter. (b) Pattern of the same emitter, showing cumulative disruption of the clean tungsten surface (just prior to vacuum arc) resulting from emission of a peak pulse current of 57 mA at 15.3 kV ($\phi = 4.52$ eV) with a duty factor of 10^{-4}. (c) Pattern of the same emitter, with an adsorbed zirconium-oxygen layer and emitting stably a peak pulse current of 102mA at 14.8kV ($\phi = 2.8$ eV for the brightly emitting areas).

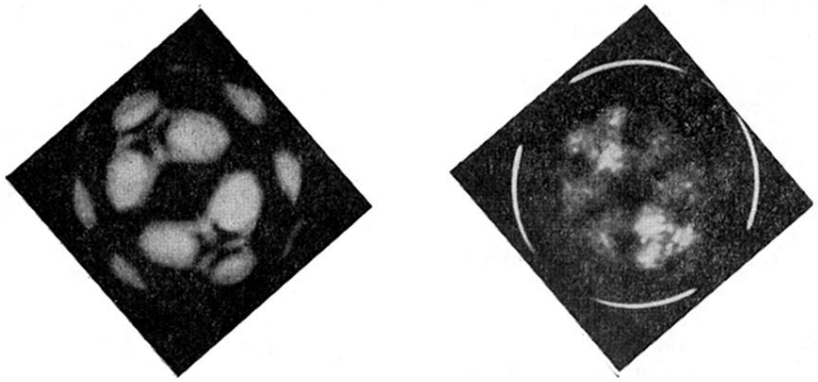

(a) (b)

FIG. 8. (a) Pulse field electron pattern of a near monolayer coverage of barium on tungsten exhibiting an average work function of 2.0 eV. Picture taken at 3.4 kV. (b) Same as pattern (a) but after emitting 84 mA of peak pulse electron current at a duty factor of 10^{-4} for 300 sec. Picture taken at 7.8 kV.

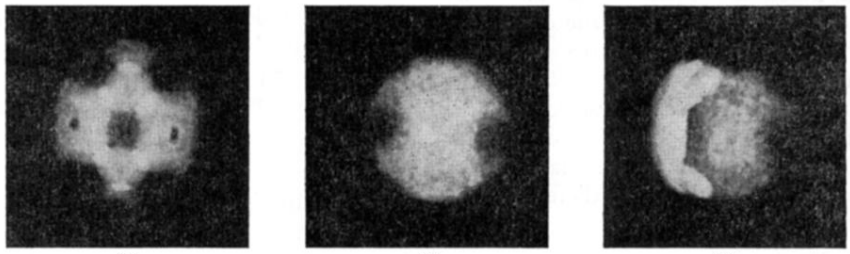

(a) (b) (c)

FIG. 9. (a) Pulse field electron pattern of a tungsten tip with cesium coverage in excess of one monolayer. The average work function of the covered surface is 1.78 eV. (b) Pattern of same tip but after emitting a peak pulse current of 53 mA (1 μsec pulses at 100 pps) for 300 sec; the coverage in the emitting region has decreased to approximately 0.5 monolayer, as determined by the work-function change to 2.1 eV. (c) Evidence of cesium migration from the heavily covered shank to the tip, produced by heating pattern (b) to 173°K for only 300 sec.